Isotope Analysis Reveals Differential Impacts of Artificial and Natural Afforestation on Soil Organic Carbon Dynamics in Abandoned Farmland

Dongrui Di (didongrui@163.com)
Sophia University: Jochi Daigaku
GuangWei Huang
Sophia University: Jochi Daigaku

Research Article

Keywords: soil carbon stock, vegetation restoration, soil aggregate, soil respiration, 13C, 14C

Posted Date: February 24th, 2021

DOI: https://doi.org/10.21203/rs.3.rs-238894/v1

Title: Isotope analysis reveals differential impacts of artificial and natural afforestation on soil organic carbon dynamics in abandoned farmland

Authors and Affiliations:

Dong-Rui Di, Guang-Wei Huang*

Graduate School of Global Environmental Studies, Sophia University, Tokyo 102-8554, Japan

Dong-Rui Di

didongrui@163.com

Guang-Wei Huang

huanggw@sophia.ac.jp

***Corresponding authors:** Guang-Wei Huang, huanggw@sophia.ac.jp

Tel/FAX: + 81-3-32384667

Abstract:

Backgrounds A multitude of studies have applied different methods to study the dynamics of soil organic carbon (SOC), but the differential impact of artificial and natural vegetation restoration on SOC dynamic are still poorly understood.

Methods and aims We investigated the SOC dynamics following artificial and natural

afforestation in Loess Plateau of China, characterizing soil structure and stoichiometry using stable isotope carbon and radiocarbon models. We aim to compare SOC dynamics under both natural and artificial afforestation and examine how soil aggregate size classes control SOC dynamics based on stoichiometry and soil respiration.

Results Total top soil SOC stocks, C:N and C:P of differently sized soil aggregates significantly increased following vegetation restoration. ^{13}C results and Radiocarbon models indicated that the SOC decomposition rate and new SOC input rate were lower under natural afforestation than artificial afforestation and revealed the highest SOC decomposition rate under natural afforestation compared to other two ecosystems.

Conclusions Vegetation restorations can accumulate SOC in top soils. Soil aggregates alternately play a dominant role in SOC accumulation following vegetation restoration; SOC loss from soil respiration was derived from microaggregates during afforestation. Recovery time is a key factor for the accumulation of SOC following afforestation.

Keywords: soil carbon stock; vegetation restoration; soil aggregate; soil respiration; ^{13}C; ^{14}C

1. Introduction

Soil contains vast and dynamic pools of organic carbon that are fundamental for maintaining the balance of atmospheric CO_2 concentrations (Lal 2004; Post et al. 1982).The soil organic carbon (SOC) pool and its dynamics are important properties of ecosystems (Schmidt et al. 2011). A multitude of studies report ecosystem changes significantly affect SOC pool and decomposition rate (Deng et al. 2016; Don et al. 2011; Snell et al. 2015; Wei et al. 2013; Zhang et al. 2015).

The Loess Plateau is the one of the largest geographic units in China. Rapid population growth combining with climate and environmental conditions in the area have resulted in severe soil erosion in the Loess Plateau (Shi et al. 2017). The Grain for Green project was implemented in 1999 to halt soil erosion and promote ecological restoration in the region. As part of this project, both natural and artificial afforestation have been promoted as methods of ecological restoration (Shi et al. 2011).

Human ecosystem interventions such as deforestation and afforestation, can cause rapid and persistent changes in vegetation and soil. Wei et al. (2013) found SOC stocks decreased most rapidly during the first 4 years of cropland cultivation after deforesting, but Rytter (2016) reported that SOC pools were generally unchanged after five years of *Salicaceae* growth during afforestation of former agricultural land. Natural change refers to the dynamic nature of ecosystem succession. Studies indicate that natural regeneration is slow and patchy with low species diversity (Blackham et al. 2014), and factors controlling SOC accumulation differed along vegetation

succession (Liu et al. 2015).

Previous studies have applied different methods (e.g. space-for-time substitution, stable isotope analysis) to study SOC dynamics and have successfully answered questions related to soil structure and organic matter dynamics (Marin-Spiotta et al. 2009; Qiu et al. 2015). However, these previous studies mainly focused on natural ecosystem restoration, without considering the effects of artificial restoration. Furthermore, although Deng et al. (2016) have investigated the SOC turnover during natural succession, SOC dynamics in stable post-succession communities (climax community) following afforestation remain unstudied.

In this study, we combined (1) a radiocarbon (^{14}C) model to estimate SOC decomposition rates in climax stage or long-term unchanged stage; (2) a natural abundance stable carbon isotope (^{13}C) study to quantify old and new carbon turnover during both natural and artificial restoration; (3) measures of change of soil aggregate-associated ecological stoichiometry to investigate the sensitivity and efficiency of soil aggregate-associated organic carbon; and (4) long-term field monitoring of soil respiration to assess SOC loss. We aim to compare SOC dynamics under both natural and artificial afforestation and examine how soil aggregate size classes control SOC dynamics based on stoichiometry and soil respiration.

2. Materials and methods

2.1. Study site

The study site consisted of semi-arid forests located on Mt. Gonglushan, near Yan'an

city in Shaanxi province, China (36°25.40″N, 109°31.53″E; 1245-1395m a.s.l.). On the Loess Plateau, precipitation and forest cover gradually decrease to the northwest, and our study site is located in the forest–grassland transition zone (Shi et al. 2014).The 40-year averages (1971-2010) of annual precipitation and annual mean air temperature were 504.7 mm and 10.1 °C, respectively (Shi et al. 2012a). The soils are classified as Calcic Cambisols, which are derived from silt textured loess parent materials (Wei et al. 2013).

2.2. Field investigation and sampling

We obtained estimates of the recovery periods of different communities from vegetation surveys from the 1950s to the early 2000s (Chen 1954; Fan et al. 2006; Zou et al. 2001) and records from local farmers and government (Tateno et al. 2007; Wang et al. 2010). These results have been accepted and used widely (Deng et al. 2013; Deng et al. 2016; Qiu et al. 2015). The study examined two different types of vegetation restoration: natural vegetation restoration from abandoned farmland to natural forest dominated by *Quercus liaotungensis* Koidz (80 years) and artificial restoration from abandoned farmland to plantation dominated by *Robinia pseudoacacia* L. (40 years). We compared these restoration types to a control site of abandoned farmland that remained unforested. The three ecosystems were at least 3km apart. To minimize the effects of area conditions on experimental results, we selected study areas with similar topography, land-use history, and soil type. Five 20 m×20 m plots were established within each ecosystem in April 2010. Each plot was at least 40 m from ecosystem boundary to minimize edge effects. Plots were spaced

111 approximately 50 m apart in each ecosystem.

112 In each plot, the litter on the ground was first removed and collected for
113 measurement. We then dug a 20 cm-deep pit in center of the plot and took three soil
114 bulk density (BD) samples. BD was measured at 0-20 cm in each subplot using a
115 stainless steel cutting ring (5×5 cm). The soil cores were dried at 105℃ for 24h.

116 Five soil samples (0-20 cm) were collected from the four corners and the center
117 of each plot, and the collected samples were mixed to form one homogeneous sample
118 for analysis of $\delta^{13}C$, ^{14}C, and aggregate size distribution. Three aggregate-size classes
119 were manually fractionated through dry sieving of fresh soil samples on a series of
120 two sieves (0.25 and 0.053mm) as follows: macroaggregates (>0.25mm),
121 microaggregates (0.25-0.053mm) and silt & clay (<0.053mm). Fresh soil samples
122 were dry sieved because wet sieving compromised the *in situ* link between the
123 aggregates obtained and their indigenous biota. Furthermore, wet sieving could cause
124 inaccurate evaluation of soil organic carbon (Jiang et al. 2014). The subsamples of
125 each aggregate fraction were used for soil organic carbon (SOC), total nitrogen (N),
126 and total phosphorous (P) analysis. Each aggregate fraction was oven dried at 100°C
127 and weighed to determine its proportion of total soil weight.

128 ***2.3. Laboratory analysis***

129 Soil organic carbon (SOC), total nitrogen (N), and total phosphorous (P) were
130 measured using a TOC VWP (Shimadzu, Japan), 2300 kjeltec analyzer unit (FOSS
131 TECATOR, Sweden), and ICP-AES (Spectro, Analytical Instruments, Germany),
132 respectively. Soil organic carbon stock was calculated as the product of soil bulk

density and SOC concentration.

Soil samples for $\delta^{13}C$ analyses were pretreated with excess 1mol L^{-1}HCl to remove carbonates at room temperature, then rinsed and freeze dried for at least 24 h and ground into fine powder over 100μm meshes. Litters was washed with distilled water, then freeze-dried and ground into fine powder for measurement. The natural abundance of $\delta^{13}C$ values in the soil organic matter and litter was analyzed with an Elemental Analyser (Eurovector) coupled to an isotope Ratio Mass Spectrometer (Delta plus, Thermo Fisher Scientific, USA) at the State key laboratory of Loess and Quaternary Geology at the Institute of Earth Environment, Chinese Academy of Sciences. Variation in the $^{13}C/^{12}C$ was reported relative to the Vienna PDB standard, and is expressed as:

$$\delta(‰) = \left(\frac{R_{sample}}{R_{standard}} - 1\right) \times 1000 \qquad (1)$$

Where R_{sample} is the $^{13}C/^{12}C$ ratio of the sample and $R_{standard}$ is the $^{13}C/^{12}C$ ratio in the PDB standard.

The soil samples were pretreated for ^{14}C analyses as follows. First, the soil samples were soaked in deionized water overnight, and then transferred to an ultrasonic bath for 30 min for completely disintegration and homogenization. The wet samples were sieved using a 180μm mesh to remove root fragments. Then, 1mol L^{-1}HCl was added to the samples, and they were placed in a water bath at 70℃ for 2 hours to remove carbonates. The samples were then rinsed repeatedly until neutral, then dried overnight in an electric oven at 60 ℃. Finally, the desiccated samples were transferred into glass vials and sealed tightly for subsequent combustion and

graphitization (Zhou et al. 1992). Measurement of ^{14}C in soil organic matter was carried out at the Xi'an Accelerator Mass Spectrometry Center in the Institute of Earth Environment, Chinese Academy of Science. Cryogenically purified CO_2 was converted to the target using the hydrogen-iron reduction method. This method was described in detail by Zhu et al. (2010).

2.4. Measurement of soil respiration

Soil respiration was measured using an automated soil CO_2 flux system (LI-8100, LI-COR, USA) equipped with a portable chamber (Model 8100-103). A PVC collar (20.3 cm in diameter and 10 cm in height) was inserted into the forest floor to a depth of 2.5 cm at each sampling point, approximately two months before the first measurements. Small litter and branches were left in the collar while large items were removed. All collars were left at the respective site for the entirety of the study period.

Soil respiration was measured over the 4-year period from 14 June 2010 to 20June 2014, approximately once every 30 days during April-October (growing season), and once every 45 days in other months (dormant season). The measurements were conducted between 8:30 and 11:30 local time on each sampling day. In each plot, five 5 m×5 m subplots were established at the four corners and the center. The PVC collars were installed in the center of each subplot for measurements of soil CO_2 efflux.

2.5. Data analysis

177 Soil OC stocks were calculated as follow:

178 $$\text{Soil } OC \text{ stocks } (kg\ m^{-2}) = \frac{D \times BD \times OC}{100} \quad (2)$$

179 Where D is the thinness (cm) of the soil layer, BD is the bulk density (g cm^{-3}), and

180 OC is the soil organic carbon concentrate (g kg^{-1}) at 0-20 cm.

181 Stocks of soil OC in each soil aggregate size class were calculated as:

182 $$\text{Stocks of } OC_i (kg\ m^{-2}) = \frac{D \times BD \times w_i \times OC_i}{10000} \quad (3)$$

183 Where OC_i is the soil organic carbon concentration of the *i*th aggregate size class (g

184 kg^{-1} aggregate).

185 During the afforestation period, the decomposition rate constants k_1(yr^{-1}) was

186 calculated by these models based on $\delta^{13}C$ method: The proportions of new SOC (f_{new})

187 and old SOC (f_{old}) were estimated based on the mass balance equations (Del Galdo et

188 al. 2003):

$$f_{new} = \frac{(\delta_{new} - \delta_{old}) \times 100\%}{\delta_{veg} - \delta_{old}} \quad (4)$$

189

190 $$f_{old} = 100 - f_{new} \quad (5)$$

191 where δ_{new} is the $\delta^{13}C$ value of the soil sample from current ecosystem, δ_{old} is the$\delta^{13}C$

192 value of the soil sample prior to ecosystem succession and δ_{veg} is the $\delta^{13}C$ value of the

193 mixed litter of current vegetation. Decomposition rate constants (k_1) of soil OC were

194 estimated using the following equations(Marin-Spiotta et al. 2009):

195 $$k_1 = \frac{-ln\ (C_t / C_0)}{t} \quad (6)$$

196 Where C_0 is the initial SOC stock (SOC stock in the reference sites), C_t is initial SOC

197 stock remaining (old C stock) at time t (year) since ecosystem change.

For the long-term or unchanged ecosystem, the decomposition rate constants k_2 (yr^{-1}) was obtained through the bomb-^{14}C model (Cherkinsky and Brovkin 1993; Torn et al. 2002; Trumbore 1993). The procedures were as follows (Tan et al. 2013):

^{14}C data (pMC) is defined as

$$pMC(\%)=\frac{A_{SN}}{A_{ON}\times e^{\lambda(y-1950)}}\times 100 \qquad (7)$$

where A_{SN} is the $^{14}C/^{12}C$ ratio of the sample corrected to a$\delta^{13}C$ value of −25‰ to account for the assumption that plants discriminate twice as much against ^{14}C as they do against ^{13}C, A_{ON} is the $^{14}C/^{12}C$ ratio of the oxalic acid activity normalized to $\delta^{13}C$ value of −19‰, λ = 1/8267 is based on the 5730 a half-life, and (y) is the year of Oxalic measurement.

The SOC turnover times were estimated using a time dependent steady-state box model. This assumes that variation in ^{14}C in a soil with time follows a first-order kinetic law, which the can be described by mass balance equation:

$$C_y\times {}^{14}C_y = C_{y\text{-}1}\times {}^{14}C_{y\text{-}1}\times(1-k_2\text{-}\lambda) + I\times {}^{14}C_{atm_{y\text{-}lag}} \qquad (8)$$

where C is the organic carbon inventory of a soil sample (g C m^{-2}), ^{14}C is the pMC of a soil sample (%), k is the first order decomposition constant for homogeneous C pools(a^{-1}), λ is the ^{14}C decay constant (1/8267), I is the annual carbon input (g C m^{-2} a^{-1}), $^{14}C_{atm}$is the pMC of the atmosphere CO_2 (%), lag is the average number of years that atmospheric CO_2 is retained in plant tissue before becoming part of the soil organic matter pool. At steady state, $C_y = C_{y-1}$and $I = kC$, eq. (7) can be transformed into:

$$^{14}C_y = {}^{14}C_{atm_{y\text{-}lag}}\times k_2 + {}^{14}C_{y\text{-}1}\times(1-k_2\text{-}\lambda) \qquad (9)$$

The decomposition rate constant k_2 is obtained by matching the modeled and measured *p*MC for the year in which the soil was sampled based on $^{14}C_{atm}$ adopt from curve of ^{14}C of atmospheric CO_2.

A method was proposed by Qiu et al. (2012) for assessing the relative contribution of changes in aggregate amount and aggregate-associated OC concentrations to the total changes in OC stocks within each aggregate fraction. It was assumed that changes in OC stock within any particular aggregate fraction were caused both by changes in OC concentration in the fraction (F_1) and by changes in the mass of the fraction (F_2). It was also assumed that the mass that was gained or lost from an aggregate fraction due to ecosystem change had the same OC concentration as the rest of that fraction after ecosystem change. We therefore calculated the contribution of F_1 and F_2 to the total change in OC stock within an aggregate fraction as follows:

$$F_1 = \mathrm{M}\times\Delta\mathrm{C} \qquad (11)$$

$$F_2 = \Delta\mathrm{M}\times\mathrm{C} \qquad (12)$$

where F_1 is the change in OC stock (g m^{-2}) within an aggregate fraction due to changes in aggregate-associated OC concentrations, F_2 is the change in the OC stock (gm^{-2}) within an aggregate fraction due to changes in the mass of the aggregate fraction, ΔM is the change in the mass of a particular fraction (kg m^{-2}), M is the initial mass of the aggregate fraction (kg m^{-2}) before ecosystem change, C is the final OC concentration of the aggregate fraction (g kg^{-1}) after ecosystem change and ΔC is the change in the OC concentration of the aggregate fraction (g kg^{-1}) due to ecosystem

change.

2.6.Calculation of Annual soil CO_2 emissions

Annual soil CO_2 emissions were estimated by interpolating the average CO_2 flux rate between sampling dates, and computing the sum of the products of the average flux rate and the time between respective sampling dates for each measurement period(Shi et al. 2014; Shi et al. 2012b; Sims and Bradford 2001)as follows:

$$R = \sum F_{m,n} \Delta t_n \qquad (13)$$

Where $\Delta t_n = t_{n+1} - t_n$, which is the number of days between each field measurement within the year; R is total soil CO_2 emitted in the measurement period, and $F_{m,n}$ is the average CO_2 flux rate over the interval $t_{n+1} - t_n$ recorded by the LI-8100 Soil CO_2 Flux System.

2.7 Statistical analyses

One-way Analysis of Variation (ANOVA) with Pearson's test was performed to examine the difference between abandoned farmland and artificial afforestation or abandoned farmland and natural afforestation in OC stocks of total soil and different soil aggregate size classes, soil aggregate size class distributions, C:N and C:P of different soil aggregate size classes, mean annual soil CO_2 emission. ANOVA also was applied to examine the different between period of artificial and natural afforestation in SOC decomposition rate constants (k_1) and new SOC input rate calculated with a ^{13}C model. Repeated measures ANOVA (RMANOVA) was applied to test the significance of SOC decomposition rate constants (k_2) calculated with a ^{14}C model among the three land use types using Tukeys's HSD test at $p< 0.05$. All

differences were evaluated at the 5% significance level.

3. Results

3.1. Total and size class aggregate OC stocks

Fig. 1 shows the change of total and different aggregate size OC stocks. Total OC stocks in top soil (0-20 cm) significantly increased with both artificial afforestation dominated by plantation of *Robinia pseudoacacia* L (AR) and natural afforestation dominated by natural forest *Quercus liaotungensis* Koidz (NQ). Nevertheless, OC sequestration following artificial afforestation was significant lower than for natural afforestation. Under both artificial and natural afforestation, the OC stocks of macroaggregates and microaggregates significantly increased , but the OC stocks of silt & clay were nearly 0 (far lower than for any other fraction), and could thus be considered a negligible part of total OC stocks (Fig 1). The OC stock of macroaggregates was significant higher than that of microaggregate in AR (Fig. 1a), but the OC stock of macroaggregate and microaggregate were nearly the same in NQ (Fig. 1b).

3.2. Aggregate size distribution and C:N & C:P in different size aggregates

Macroaggregates and microaggregates accounted for approximate 99 % of the dry soil weight in the abandoned farmland. Under both artificial and natural restoration, the amount of soil in macroaggregates significantly increased, and microaggreagtes significantly decreased (Fig 2). Furthermore, for both types of restorations, the amount of soils in silt & clay was less than 1% and did not

286 significantly change.

287 Both C:N and C:P of different aggregate classes significantly increased with both
288 types of vegetation restoration. Compared with other size aggregates, C:N and C:P of
289 microaggregates become higher after restoration (Fig 3).

290 ***3.3. Turnover of SOC under artificial and natural afforestation***

291 Over the vegetation restoration period, the SOC decomposition rate (k_1), and
292 new SOC input rate under artificial restoration were higher than natural restoration
293 (Fig 4). For climax or long-term unchanged stage, the SOC decomposition rate (k_2)
294 was highest (2.6×10^{-3}) in the natural forest ecosystem (*Quercus liaotungensis* Koidz).
295 The k_2 of abandoned farmland and plantation (*Robinia pseudoacacia* L.) were similar
296 (Fig 5).

297 ***3.4. Amount of soil CO_2 emissions***

298 The amount of soil CO_2 emissions across ecosystems was calculated from
299 continuous measurements over 4 years. Both natural and artificial restoration
300 significantly increased the amount of soil CO_2 emissions, and the increased of amount
301 of soil CO_2 emissions was higher under natural restoration than artificial restoration
302 (Fig 6).

303

304 **4. Discussion**

305 A multitude of studies found that vegetation restoration can lead to the
306 accumulation of SOC, and the effects of land use change during vegetation restoration
307 on soil OC are mainly due to changes in OC input and C mineralization (Deng et al.

2016; Laganiére et al. 2010). The OC in soil physical fractions responds more sensitively and rapidly to land use change than the OC in bulk soils (Qiu et al. 2012; Wei et al. 2013); therefore, changes in aggregate-associated OC are regarded as fundamental processes for understanding the effects of vegetation restoration on SOC.

In this study, we also found that both types of restorations could accumulate SOC in top soil (Fig 1). Our study showed that changes in F_1 & F_2 under artificial and natural restoration were nearly the same, and F_1 and F_2 significantly increased and decreased respectively, for macroaggregate-OC after afforestation, but changes in F_1 & F_2 for macroaggregate-OC were more significant under natural afforestation (Fig 7 a, b). In addition, F_1 significantly increased and F_2 slightly decreased for microaggregate-OC (Fig 7 c, d).

The model results indicated that increases in SOC stocks in macroaggregates and microaggregates under artificial and natural afforestation were mainly due to increases in SOC concentration rather than mass (Fig 7). The contribution of macroaggregate-OC concentration increases under natural afforestation was more significant than under artificial, but microaggregate-OC changes under natural and artificial afforestation were similar. Therefore, we concluded that macroaggregate-OC stock is the main contributing factor to changes in total OC stock. Qiu et al. (2015) obtained a similar result. Nevertheless, under artificial afforestation we found that OC stocks in macroaggregates and microaggregates equally contributed to the dynamics of total OC stocks.

Meanwhile, we found that soil respiration was the main pathway of soil OC loss.

330 We found that long-term soil CO_2 emission during afforestation promoted SOC loss
331 via soil respiration. Spohn and Chodak (2015) demonstrated that microorganisms
332 increase their respiration rate with an increase in soil C/P ratio and C concentration. In
333 this study, we found that C/N and C/P ratios in microaggregates were consistently
334 higher than in other fractions under afforestation (Fig 3). Therefore, it was concluded
335 that SOC loss from soil respiration was mainly originated from microaggregate
336 resulting from higher C/P ratio after afforestation, supporting the previous inference in
337 terms of relationship between ecological stoichiometry and soil respiration.

338 Moreover, although our study found higher SOC accumulation under natural
339 afforestation than under artificial afforestation (Fig 1), and the increase in proportion
340 of new OC in soils could be attributed to the OC inputs from the recent afforestation,
341 which produced organic matter with different $^{13}C/^{12}C$ ratios (Marin-Spiotta et al.
342 2009), based on analysis of ^{13}C we found old C decomposition and new C inputs
343 during natural afforestation were significantly lower than during artificial
344 afforestation (Fig 4). Previous studies focused on the process of old C decomposition
345 and new C input: Zhang et al. (2015) proposed the relationship between SOC
346 decomposition and new & old litter input, and Richter et al. (1999) reported that the
347 rates of new soil OC increase represented the net effect of new OC input and output to
348 soil. However, time since land use change has not been considered as a key parameter
349 for the accumulation of SOC. In this study, the period of natural afforestation was
350 twice as long as the period of artificial afforestation. Though the new SOC input rate
351 under natural afforestation was lower compared to artificial afforestation, the

352 decomposition rate under natural afforestation was also lower, which may indicate
353 higher SOC accumulation under natural afforestation is not attributable only to higher
354 net increases in the difference between new SOC input and old SOC decomposition.
355 We could conclude that time since land use change is a more important factor
356 determining the proportions of new and old OC in soil. Previous studies lend support
357 to this hypothesis (Deng et al. 2016; Marin-Spiotta et al. 2009)

358 Not only climax forest but also other types of ecosystems in semiarid or arid
359 region often maintain in stable stage for a long time (Fan et al. 2006) and the
360 dynamics of SOC in the ecosystem could be considered as an ecosystem property
361 (Schmidt et al. 2011). ^{14}C dating has been proven to be an ideal tool to study the
362 dynamics of SOC from decadal to millennial timescales, which provides a direct
363 measure of the time elapsed since carbon in organic matter was fixed from the
364 atmosphere (Trumbore 1993). In this study, the steady-state box model of ^{14}C of SOC
365 was applied to estimate the mean residence time (MRT) of SOC for the long-term or
366 unchanged ecosystem, providing a sensitive indicator to quantify the proportion of
367 SOC derived from the atmosphere in recent years to centuries based on the rate of
368 incorporation of the nuclear explosion before 1960s carbon tracer (Laskar et al. 2016;
369 Torn et al. 2009). In our study, the result of the ^{14}C model suggested that the carbon
370 decomposition rate was the lowest in the plantation (*Robinia pseudoacacia* L.)
371 ecosystem, and was the same as abandoned farmland. The carbon turnover was
372 highest in the natural forest ecosystem (*Quercus liaotungensis* Koidz) (Fig 5). The
373 model provided a direct evidence that higher accumulation of SOC under natural

afforestation can be attributed to its longer restoration period rather than more rapid carbon turnover under natural afforestation compared to artificial afforestation. Therefore, our study suggests that longer restoration time could be more important for SOC accumulation following afforestation than any particular method of afforestation.

5. Conclusions

In conclusion, we found that both artificial and natural afforestation promoted the accumulation of SOC in top soil, and accumulation of SOC under natural afforestation was higher than under artificial afforestation. The SOC concentration of soil aggregates played a dominant role in determining the dynamics of SOC accumulation following vegetation restoration. According to analysis of soil aggregates, soil respiration, and aggregate stoichiometry, we concluded that SOC loss from soil respiration mainly originated from microaggregates during restoration. ^{13}C and ^{14}C models proved effective tools that showed that recovery time is a key factor determining the accumulation of SOC following afforestation.

Acknowledgements

We would like to thank Dr. Julia Monk at Yale University for her assistance with English language and grammatical editing. This research has been supported by projects from Engineered Food Production for Sustainable Agriculture Systems,

396 Grand-in Aid for Challenging Research (Pioneering, No.20K20358).

397

398

399 **References**

400 Blackham GV, Webb EL, Corlett RT (2014) Natural regeneration in a degraded
401 tropical peatland, Central Kalimantan, Indonesia: Implications for forest
402 restoration. Forest Ecol Manag 324: 8-15. doi:
403 http://dx.doi.org/10.1016/j.foreco.2014.03.041.
404 Chen C (1954) The vegetation and its roles in soil and water conservation in the
405 secondary forest area in the boundary of Shaanxi and Gansu provinces. Acta
406 Phytoecologica et Geobotanica Sinica (in Chinese)(2): 152-223.
407 Cherkinsky AE, Brovkin VA (1993) Dynamics of radiocarbon in soils. Radiocarbon
408 35: 363-367.
409 Del Galdo I, Six J, Peressotti A, Francesca Cotrufo M (2003) Assessing the impact of
410 land-use change on soil C sequestration in agricultural soils by means of
411 organic matter fractionation and stable C isotopes. Global Change Biol 9:
412 1204-1213. doi: 10.1046/j.1365-2486.2003.00657.x.
413 Deng L, Wang K-B, Chen M-L, Shangguan Z-P, Sweeney S (2013) Soil organic
414 carbon storage capacity positively related to forest succession on the Loess
415 Plateau, China. CATENA 110: 1-7. doi:
416 http://dx.doi.org/10.1016/j.catena.2013.06.016.
417 Deng L, Wang K, Tang Z, Shangguan Z (2016) Soil organic carbon dynamics

following natural vegetation restoration: Evidence from stable carbon isotopes (δ13C). Agriculture Ecosyst Environ 221: 235-244. doi: http://dx.doi.org/10.1016/j.agee.2016.01.048.

Don A, Schumacher J, Freibauer A (2011) Impact of tropical land-use change on soil organic carbon stocks - a meta-analysis. Global Change Biol 17: 1658-1670. doi: 10.1111/j.1365-2486.2010.02336.x.

Fan W-Y, Wang X-A, Guo H (2006) Analysis of plant community successional series in the Ziwuling area on the Loess Plateau. Acta Ecologica Sinica 26: 706-714.

Jiang Y, Jin C, Sun B (2014) Soil aggregate stratification of nematodes and ammonia oxidizers affects nitrification in an acid soil. Environ Microbiol 16: 3083-3094. doi: 10.1111/1462-2920.12339.

Laganiére J, Angers DA, ParÉ D (2010) Carbon accumulation in agricultural soils after afforestation: a meta-analysis. Global Change Biol 16: 439-453. doi: 10.1111/j.1365-2486.2009.01930.x.

Lal R (2004) Soil carbon sequestration impacts on global climate change and food security. Science 304: 1623-1627. doi: 10.1126/science.1097396.

Laskar AH, Yadava MG, Ramesh R (2016) Radiocarbon and Stable Carbon Isotopes in Two Soil Profiles from Northeast India. Radiocarbon 54: 81-89. doi: 10.2458/azu_js_rc.v54i1.15840.

Liu S, Zhang W, Wang K, Pan F, Yang S, Shu S (2015) Factors controlling accumulation of soil organic carbon along vegetation succession in a typical karst region in Southwest China. Sci Total Environ 521–522: 52-58. doi:

http://dx.doi.org/10.1016/j.scitotenv.2015.03.074.

Marin-Spiotta E, Silver WL, Swanston CW, Ostertag R (2009) Soil organic matter dynamics during 80 years of reforestation of tropical pastures. Global Change Biol 15: 1584-1597. doi: 10.1111/j.1365-2486.2008.01805.x.

Post WM, Emanuel WR, Zinke PJ, Stangenberger AG (1982) Soil carbon pools and world life zones. Nature 298: 156-159. doi: 10.1038/298156a0.

Qiu L, Wei X, Zhang X, Cheng J, Gale W, Guo C, Long T (2012) Soil organic carbon losses due to land use change in a semiarid grassland. Plant Soil 355: 299-309. doi: 10.1007/s11104-011-1099-x.

Qiu LP, Wei XR, Gao JL, Zhang XC (2015) Dynamics of soil aggregate-associated organic carbon along an afforestation chronosequence. Plant Soil 391: 237-251. doi: 10.1007/s11104-015-2415-7.

Richter DD, Markewitz D, Trumbore SE, Wells CG (1999) Rapid accumulation and turnover of soil carbon in a re-establishing forest. Nature 400: 56-58. doi: 10.1038/21867.

Rytter RM (2016) Afforestation of former agricultural land with Salicaceae species - Initial effects on soil organic carbon, mineral nutrients, C:N and pH. Forest Ecol Manag 363: 21-30. doi: 10.1016/j.foreco.2015.12.026.

Schmidt MWI, Torn MS, Abiven S, Dittmar T, Guggenberger G, Janssens IA, Kleber M, Kogel-Knabner I, Lehmann J, Manning DAC, Nannipieri P, Rasse DP, Weiner S, Trumbore SE (2011) Persistence of soil organic matter as an ecosystem property. Nature 478: 49-56. doi: 10.1038/nature10386.

462 Shi WY, Du S, Morina JC, Guan JH, Wang KB, Ma MG, Yamanaka N, Tateno R
463 (2017) Physical and biogeochemical controls on soil respiration along a
464 topographical gradient in a semiarid forest. Agr Forest Meteorol 247: 1-11. doi:
465 10.1016/j.agrformet.2017.07.006.
466 Shi WY, Tateno R, Zhang JG, Wang YL, Yamanaka N, Du S (2011) Response of soil
467 respiration to precipitation during the dry season in two typical forest stands in
468 the forest-grassland transition zone of the Loess Plateau. Agr Forest Meteorol
469 151: 854-863. doi: 10.1016/j.agrformet.2011.02.003.
470 Shi WY, Yan MJ, Zhang JG, Guan JH, Du S (2014) Soil CO2 emissions from five
471 different types of land use on the semiarid Loess Plateau of China, with
472 emphasis on the contribution of winter soil respiration. Atmos Environ 88:
473 74-82. doi: 10.1016/j.atmosenv.2014.01.066.
474 Shi WY, Zhang JG, Yan MJ, Yamanaka N, Du S (2012a) Seasonal and diurnal
475 dynamics of soil respiration fluxes in two typical forests on the semiarid Loess
476 Plateau of China: Temperature sensitivities of autotrophs and heterotrophs and
477 analyses of integrated driving factors. Soil Biol Biochem 52: 99-107. doi:
478 10.1016/j.soilbio.2012.04.020.
479 Shi XH, Zhang XP, Yang XM, Drury CF, McLaughlin NB, Liang AZ, Fan RQ, Jia SX
480 (2012b) Contribution of winter soil respiration to annual soil CO_2 emission in
481 a Mollisol under different tillage practices in northeast China (Vol 26, GB2007,
482 doi: 2011GB004054). Glob Biogeochem Cycle 26: GB3020. doi:
483 10.1029/2012gb004477.

484 Sims PL, Bradford JA (2001) Carbon dioxide fluxes in a southern plains prairie. Agr
485 Forest Meteorol 109: 117-134. doi:
486 http://dx.doi.org/10.1016/S0168-1923(01)00264-7.
487 Snell HSK, Robinson D, Midwood AJ (2015) Tree species' influences on soil carbon
488 dynamics revealed with natural abundance 13C techniques. Plant Soil 400:
489 285-296. doi: 10.1007/s11104-015-2731-y.
490 Spohn M, Chodak M (2015) Microbial respiration per unit biomass increases with
491 carbon-to-nutrient ratios in forest soils. Soil Biol Biochem 81: 128-133. doi:
492 http://dx.doi.org/10.1016/j.soilbio.2014.11.008.
493 Tan W, Zhou L, Liu K (2013) Soil aggregate fraction-based 14C analysis and its
494 application in the study of soil organic carbon turnover under forests of
495 different ages. Chinese Sci Bull 58: 1936-1947. doi:
496 10.1007/s11434-012-5660-7.
497 Tateno R, Tokuchi N, Yamanaka N, Du S, Otsuki K, Shimamura T, Xue Z, Wang S,
498 Hou Q (2007) Comparison of litterfall production and leaf litter decomposition
499 between an exotic black locust plantation and an indigenous oak forest near
500 Yan'an on the Loess Plateau, China. Forest Ecol Manag 241: 84-90. doi:
501 http://dx.doi.org/10.1016/j.foreco.2006.12.026.
502 Torn MS, Lapenis AG, Timofeev A, Fischer ML, Babikov BV, Harden JW (2002)
503 Organic carbon and carbon isotopes in modern and 100-year-old-soil archives
504 of the Russian steppe. Global Change Biol 8: 941-953. doi:
505 10.1046/j.1365-2486.2002.00477.x.

506 Torn MS, Swanston CW, Castanha C, Trumbore SE (2009) Storage and Turnover of
507 Organic Matter in Soil. Biophysico‐Chemical Processes Involving Natural
508 Nonliving Organic Matter in Environmental Systems.
509 Trumbore SE (1993) Comparison of carbon dynamics in tropical and temperate soils
510 using radiocarbon measurements. Glob Biogeochem Cycle 7: 275-290. doi:
511 10.1029/93gb00468.
512 Wang K, Shao R, Shangguan Z (2010) Changes in spicies richness and community
513 productivty during succession on the Loess Plateau(China). Pol J Ecol 58:
514 501-510.
515 Wei XR, Shao MG, Gale WJ, Zhang XC, Li LH (2013) Dynamics of
516 aggregate-associated organic carbon following conversion of forest to
517 cropland. Soil Biol Biochem 57: 876-883. doi: 10.1016/j.soilbio.2012.10.020.
518 Zhang KR, Dang HS, Zhang QF, Cheng XL (2015) Soil carbon dynamics following
519 land-use change varied with temperature and precipitation gradients: evidence
520 from stable isotopes. Global Change Biol 21: 2762-2772. doi:
521 10.1111/gcb.12886.
522 Zhou WJ, An ZS, Lin BH, Xiao JL, Zhang JZ, Xie J, Zhou MF, Porter SC, Head MJ,
523 Donahue DJ (1992) Chronology of the baxie loess profile and the history of
524 monsoon climates in China between 17000 and 6000 years BP. Radiocarbon
525 34: 818-825.
526 Zhu YZ, Cheng P, Yu SY, Yu HG, Kang ZH, Yang YC, Jull AJT, Lange T, Zhou WJ
527 (2010) Establishing a firm chronological framwork for neolithic and early

528 dynastic archaeology in the shangluo area, central China. Radiocarbon 52:
529 466-478.
530 Zou H, Liu G, Wang H (2001) The vegetation development in North Ziwulin forest
531 region in last fifty years. Acta Botanica Boreali-Occidentalia Sinica 22: 1-8.
532

533 Figure captions

534 Fig 1 Changes in OC stocks of total soil and different soil aggregate size classes under
535 (a) artificial and (b) natural afforestation. Macroaggregates were >0.25 mm;
536 microaggregates were between 0.25 and 0.053 mm; and silt & clay were <0.053 mm.
537 Error bars represent the standard error of the mean. Significant differences are
538 indicated by the asterisk symbol (*p < 0.05); ns: no significant; AF: abandoned
539 farmland; AR: artificial afforestation (plantation of *Robinia pseudoacacia* L); NQ:
540 natural afforestation (natural forest - *Quercus liaotungensis* Koidz).

541

542 Fig 2 Changes in soil aggregate size class distributions with afforestation under (a)
543 artificial and (b) natural restoration. Macroaggregates were >0.25 mm;
544 microaggregatew were between0.25 and 0.053 mm; and silt & clay were <0.053 mm.
545 Error bars represent the standard error of the mean. Significant differences are
546 indicated by the asterisk symbol (*p < 0.05); ns: no significant; AF: abandoned
547 farmland; AR: artificial afforestation (plantation of *Robinia pseudoacacia* L); NQ:
548 natural afforestation (natural forest - *Quercus liaotungensis* Koidz).

549

550 Fig 3 Changes in C:N and C:P of different soil aggregate size classes with
551 afforestation under (a-b) artificial and (c-d) natural restoration. Macroaggregates
552 were >0.25 mm; microaggregatew were between0.25 and 0.053 mm; and silt & clay
553 were <0.053 mm. Error bars represent the standard error of the mean. Significant
554 differences are indicated by the asterisk symbol (*p < 0.05); ns: no significant; AF:

555 abandoned farmland; AR: artificial afforestation (plantation of *Robinia pseudoacacia*
556 L); NQ: natural afforestation (natural forest - *Quercus liaotungensis* Koidz).
557
558 Fig 4 SOC decomposition rate constants (k_1) and new SOC input rate (kg m^{-2} yr^{-1})
559 calculated with a ^{13}C model under (a) artificial and (b) natural afforestation. Error bars
560 represent the standard error of the mean. Significant differences are indicated by the
561 asterisk symbol (*$p < 0.05$).
562
563 Fig 5 SOC decomposition rate constants (k_2) calculated with a ^{14}C model for different
564 land use types. Error bars represent the standard error of the mean. Significant
565 differences are indicated by different letters ($p < 0.05$). AF: abandoned farmland; AR:
566 artificial afforestation (plantation of *Robinia pseudoacacia* L); NQ: natural
567 afforestation (natural forest - *Quercus liaotungensis* Koidz).
568
569 Fig 6 Changes in mean annual soil CO_2 emission over 4 years of vegetation
570 restoration under (a) artificial and (b) natural afforestation. Error bars represent the
571 standard error of the mean. Significant differences are indicated by the asterisk
572 symbol (*$p < 0.05$); ns: no significant; AR: artificial afforestation (plantation of
573 *Robinia pseudoacacia* L); NQ: natural afforestation (natural forest - *Quercus*
574 *liaotungensis* Koidz).
575
576 Fig 7 Changes in SOC stocks in macroaggregates and microaggregates with

afforestation under (a-b) artificial and (c-d) natural restoration. Macroaggregates were >0.25 mm; microaggregatew were between0.25 and 0.053 mm; and silt & clay were <0.053 mm. Error bars represent the standard error of the mean. Significant differences are indicated by the asterisk symbol (*p < 0.05). AF: abandoned farmland; AR: artificial afforestation (plantation of *Robinia pseudoacacia* L); NQ: natural afforestation (natural forest - *Quercus liaotungensis* Koidz).

Figures

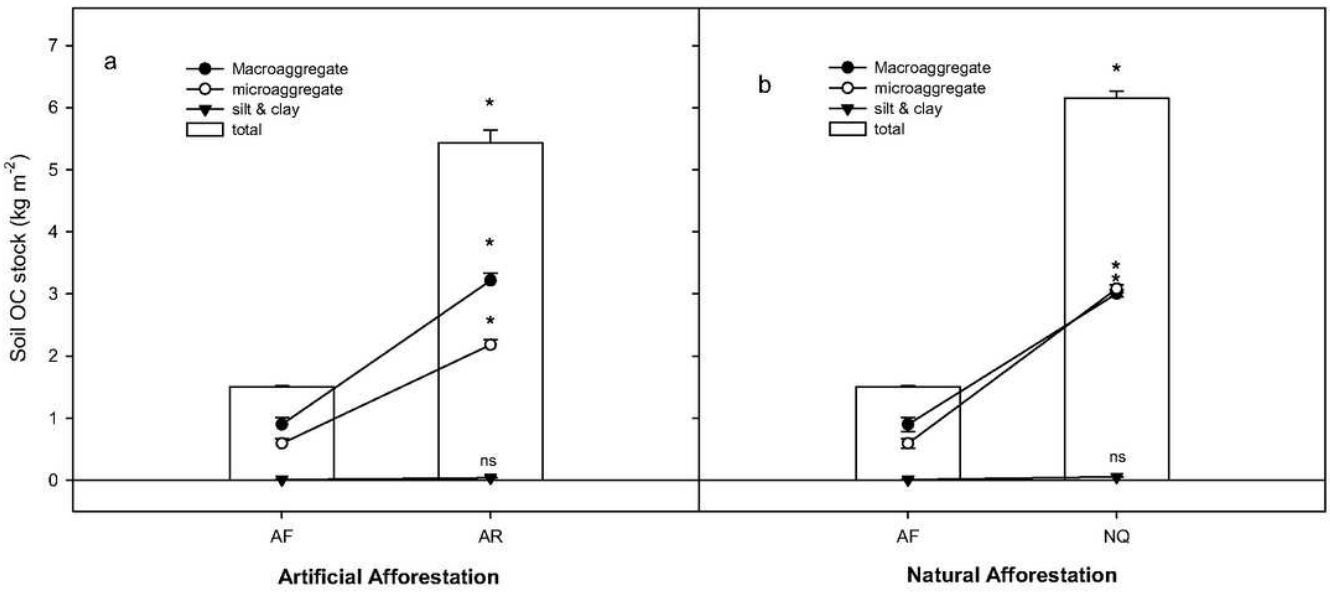

Figure 1

Changes in OC stocks of total soil and different soil aggregate size classes under (a) artificial and (b) natural afforestation. Macroaggregates were >0.25 mm; microaggregates were between 0.25 and 0.053 mm; and silt & clay were <0.053 mm. Error bars represent the standard error of the mean. Significant differences are indicated by the asterisk symbol (*p < 0.05); ns: no significant; AF: abandoned farmland; AR: artificial afforestation (plantation of Robinia pseudoacacia L); NQ: natural afforestation (natural forest - Quercus liaotungensis Koidz).

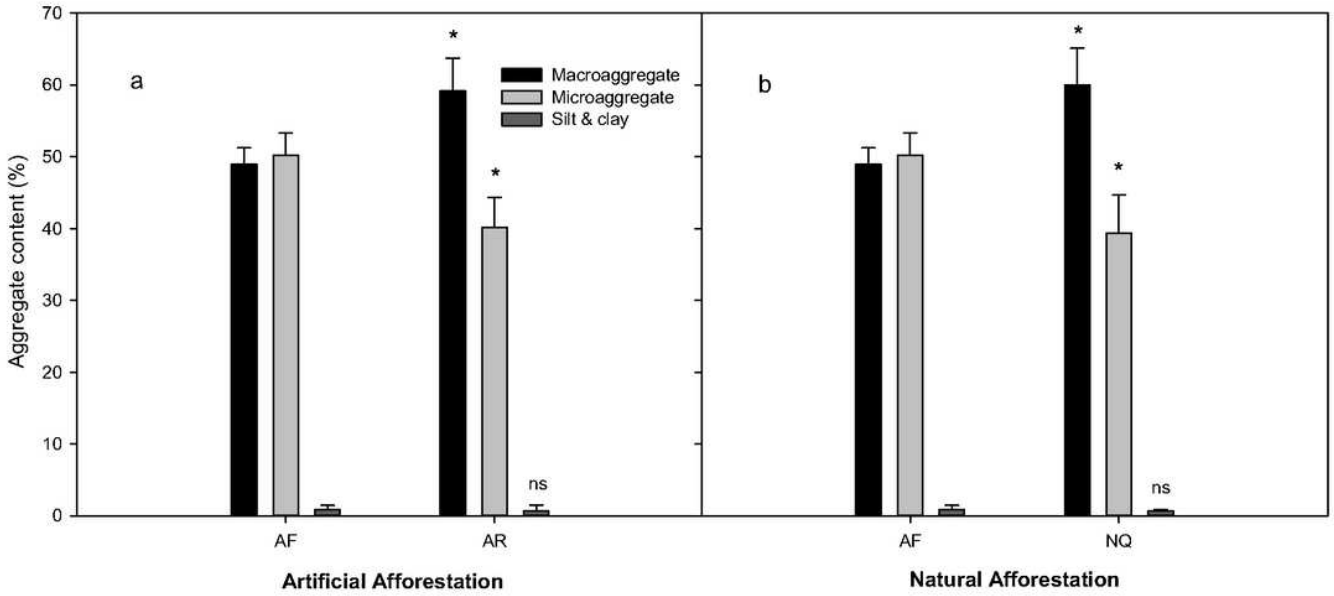

Figure 2

Changes in soil aggregate size class distributions with afforestation under (a) artificial and (b) natural restoration. Macroaggregates were >0.25 mm; microaggregatew were between0.25 and 0.053 mm; and silt & clay were <0.053 mm. Error bars represent the standard error of the mean. Significant differences are indicated by the asterisk symbol (*p < 0.05); ns: no significant; AF: abandoned farmland; AR: artificial afforestation (plantation of Robinia pseudoacacia L); NQ: natural afforestation (natural forest - Quercus liaotungensis Koidz).

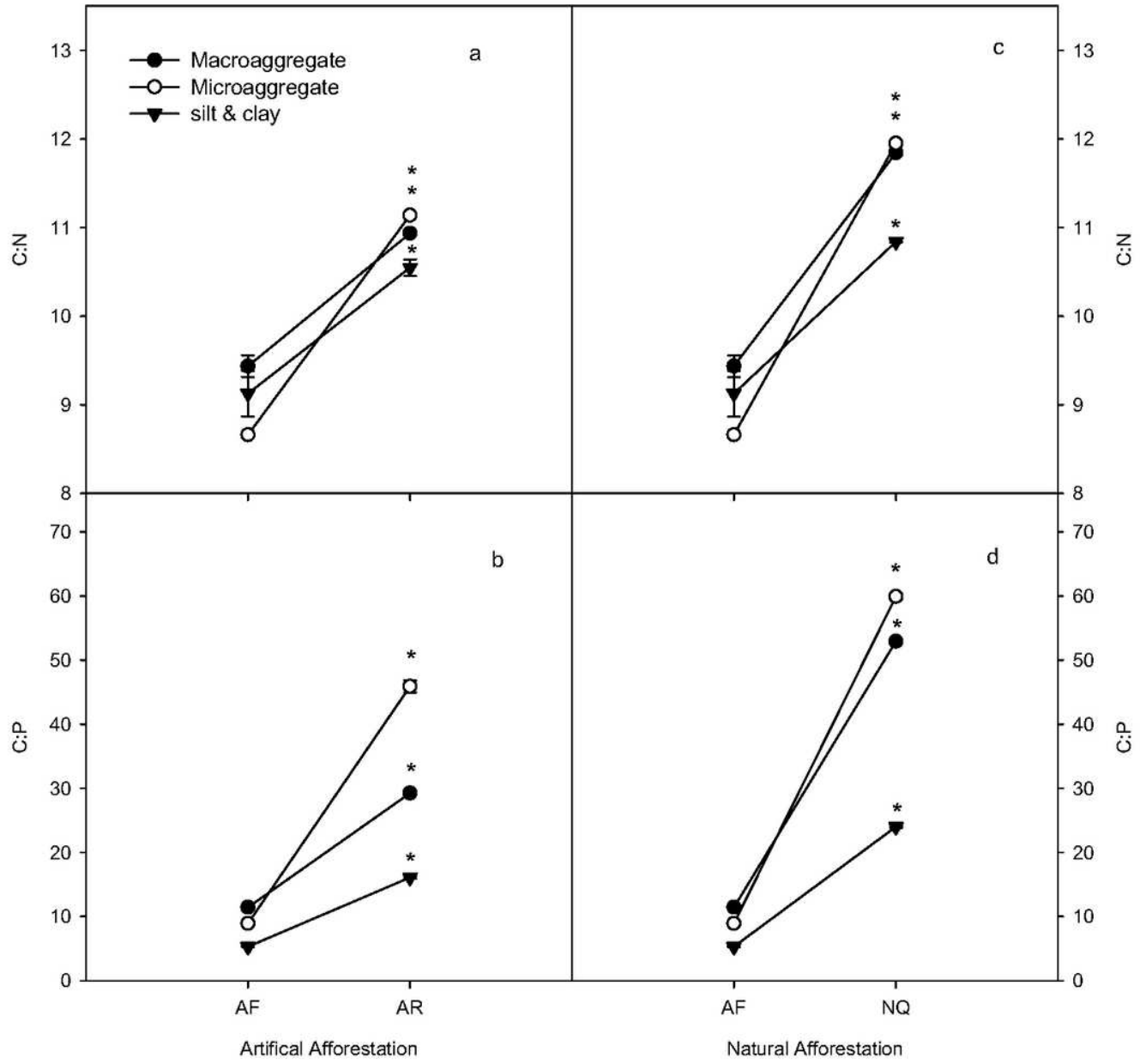

Figure 3

Changes in C:N and C:P of different soil aggregate size classes with afforestation under (a-b) artificial and (c-d) natural restoration. Macroaggregates were >0.25 mm; microaggregatew were between0.25 and 0.053 mm; and silt & clay were <0.053 mm. Error bars represent the standard error of the mean. Significant differences are indicated by the asterisk symbol (*p < 0.05); ns: no significant; AF: abandoned farmland; AR: artificial afforestation (plantation of Robinia pseudoacacia L); NQ: natural afforestation (natural forest - Quercus liaotungensis Koidz).

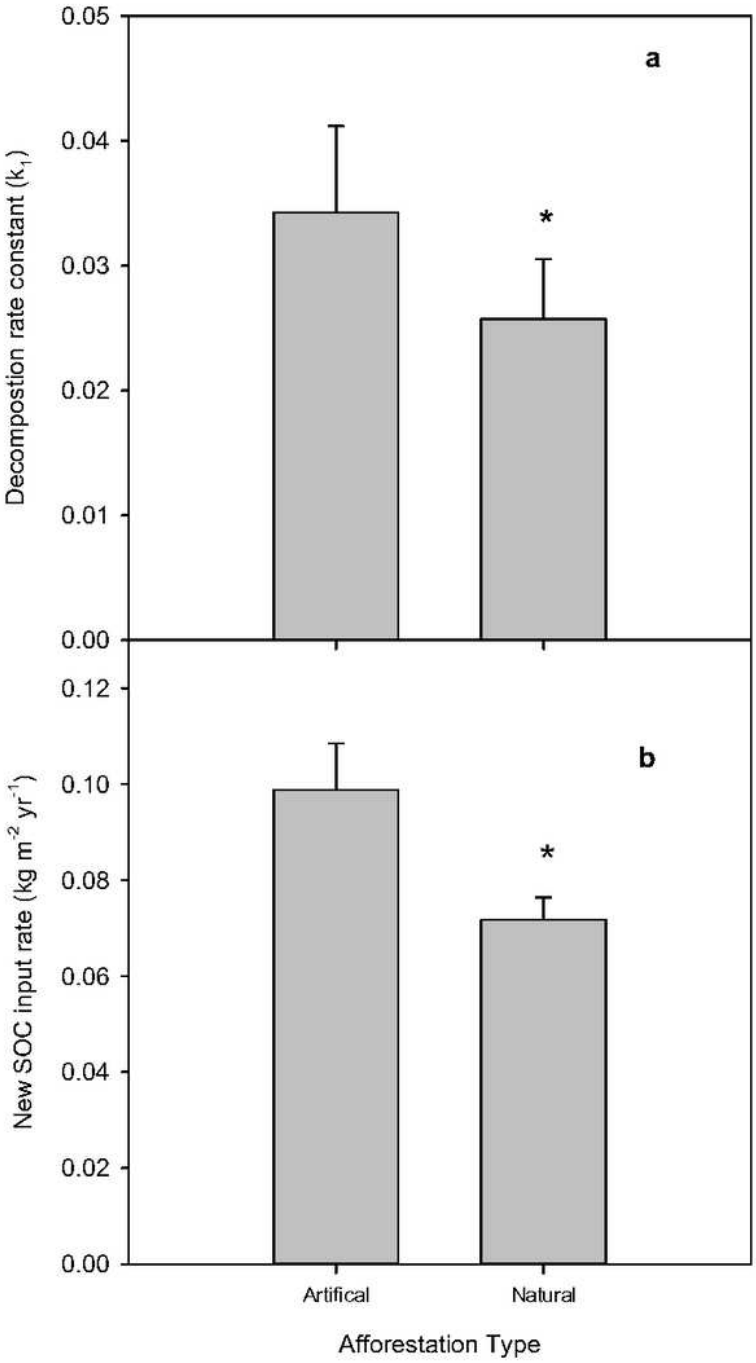

Figure 4

SOC decomposition rate constants (k1) and new SOC input rate (kg m-2 yr-1) calculated with a 13C model under (a) artificial and (b) natural afforestation. Error bars represent the standard error of the mean. Significant differences are indicated by the asterisk symbol (*p < 0.05).

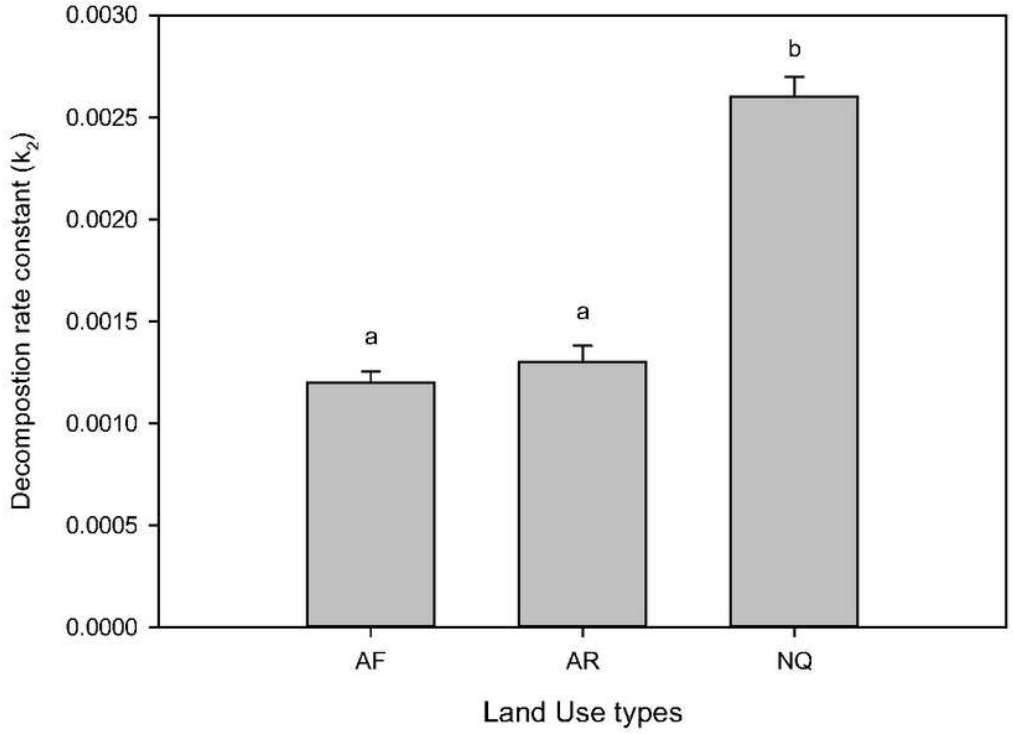

Figure 5

SOC decomposition rate constants (k2) calculated with a 14C model for different land use types. Error bars represent the standard error of the mean. Significant differences are indicated by different letters ($p < 0.05$). AF: abandoned farmland; AR: artificial afforestation (plantation of Robinia pseudoacacia L); NQ: natural afforestation (natural forest - Quercus liaotungensis Koidz).

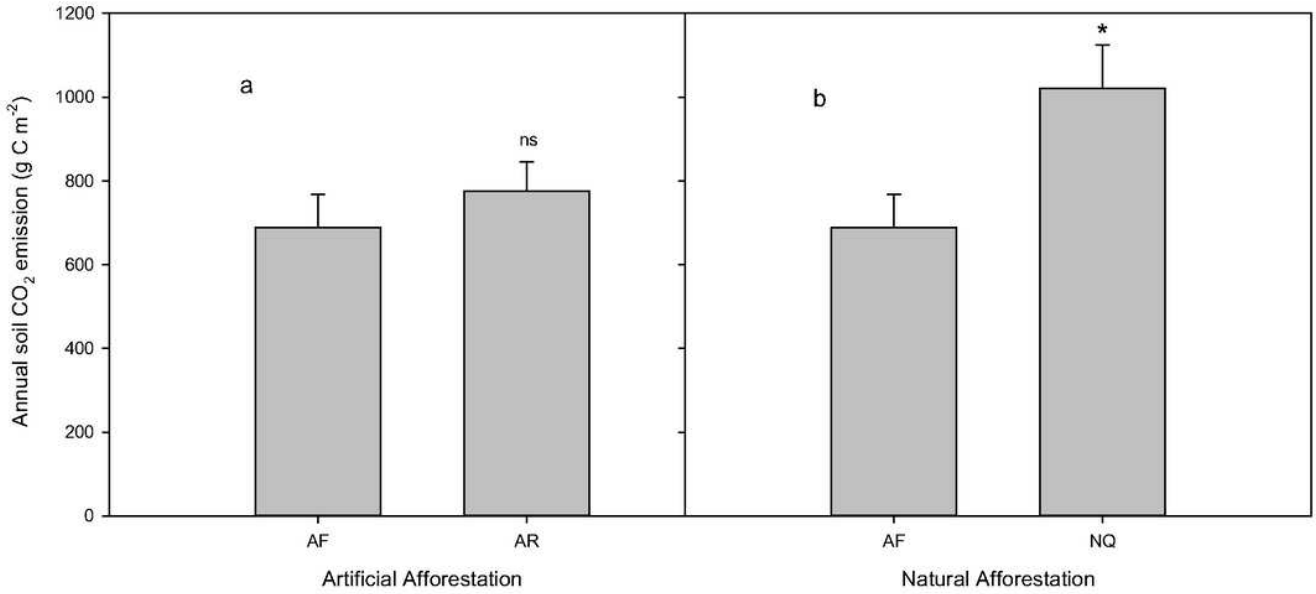

Figure 6

Changes in mean annual soil CO2 emission over 4 years of vegetation restoration under (a) artificial and (b) natural afforestation. Error bars represent the standard error of the mean. Significant differences are indicated by the asterisk symbol (*p < 0.05); ns: no significant; AR: artificial afforestation (plantation of Robinia pseudoacacia L); NQ: natural afforestation (natural forest - Quercus liaotungensis Koidz).

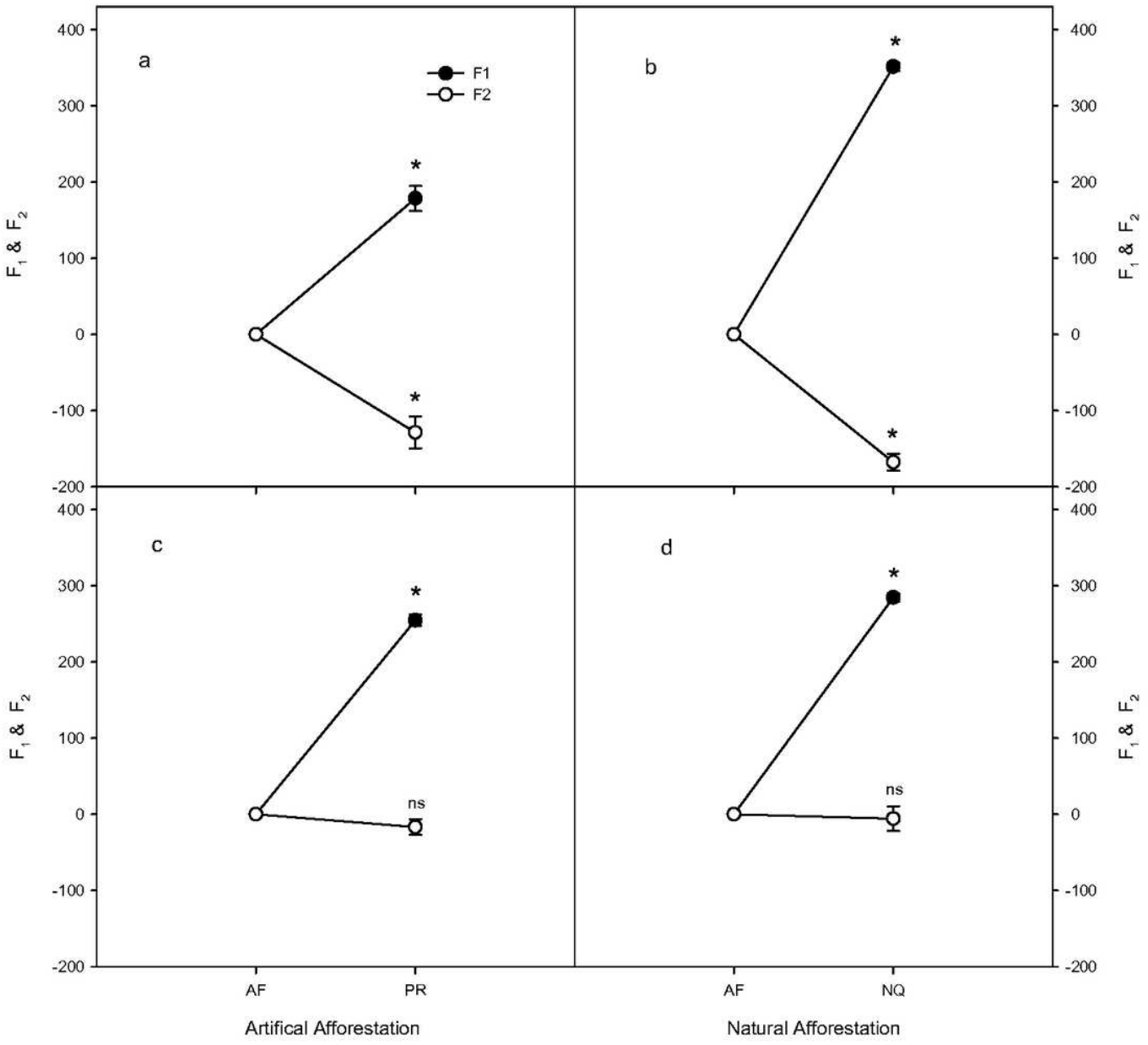

Figure 7

Changes in SOC stocks in macroaggregates and microaggregates with afforestation under (a-b) artificial and (c-d) natural restoration. Macroaggregates were >0.25 mm; microaggregatew were between0.25 and 0.053 mm; and silt & clay were <0.053 mm. Error bars represent the standard error of the mean. Significant differences are indicated by the asterisk symbol (*p < 0.05). AF: abandoned farmland; AR: artificial afforestation (plantation of Robinia pseudoacacia L); NQ: natural afforestation (natural forest - Quercus liaotungensis Koidz).